



# Matrix Backward Forward Sweep for Unbalanced Power Flow in $\alpha\beta 0$ frame<sup>☆</sup>

Cristina-González-Morán<sup>a,\*</sup>, Pablo Arbolea<sup>a</sup>, Bassam Mohamed<sup>a</sup>

<sup>a</sup>*Department of Electrical Engineering, University of Oviedo*

---

## Abstract

A Backward/Forward Sweep (BFS) algorithm for power flow calculations adapted to matrix formulation in the  $\alpha\beta 0$  reference frame is presented in this paper. The novelty of the work is the definition of a BFS solver with the following characteristics: matrix formulation in  $\alpha\beta 0$  frame, valid for unbalanced three phase or single phase systems and capable of handling transformers and distributed generators; Slack, PQ or PV nodes. The matrix formulation avoids the difficulties of load-flow methods presented in the literature: lack of generalization for arbitrary network topologies and transformer connections; the  $\alpha\beta 0$  stationary reference frame makes the algorithm easily applicable to distribution systems; and finally, the BFS algorithm is an efficient, robust and fast solver. The IEEE Node Test Feeders will be used to provide test systems under several configurations. Comparison to a direct algorithm will demonstrate the improvements in robustness, efficiency and computation time.

**Keywords:** Backward/Forward Sweep (BFS), Distributed Systems, Three-phase Unbalanced Power Flow, Transformer Modeling,  $\alpha\beta 0$  Stationary Reference Frame.

---

## 1. Introduction

The steady-state analysis of distributed systems has been a major concern in power systems operation and planning for many years. Highly efficient load flow algorithms, capable of modeling and analyzing arbitrary topologies of large-scale systems, as well as providing accurate results, are required both in transmission and distribution systems. The power flow is of special interest at medium and low voltage levels because the varying nature of distributed systems is constantly demanding algorithms that reflect on such changes [1, 2].

Traditional power flow approaches, valid for transmission levels, do not usually yield the same simplifications at distribution levels due to their special characteristics [3, 4, 5]: radial topology, relatively long untransposed lines, unbalanced loads and large number of nodes and lines. Besides these differences, the increase of distributed generation (DG), including DG controls working under unbalanced conditions [6, 7, 8] is also changing the load flow definition [4, 9, 10]. Summarizing, the load flow for distribution must contemplate several features:

- The nature of loading requires three phase unbalanced power flows. The equivalent one line with sequence networks used in transmission can not be applied to distribution. Instead, an exact line model is needed [11].

---

<sup>☆</sup>This work has been supported by the Research, Technological Development and Innovation Program Oriented to the Society Challenges of the Spanish Ministry of Economy and Competitiveness under Grant ENE2013-44245-R and by the Government of the Principality of Asturias under grant FC-15-GRUPIN14-127.

\*Corresponding author

Email addresses: [gonzalezmorcristina@uniovi.es](mailto:gonzalezmorcristina@uniovi.es) (Cristina-González-Morán), [arboleypablo@uniovi](mailto:arboleypablo@uniovi) (Pablo Arbolea), [engbassam@gmail.com](mailto:engbassam@gmail.com) (Bassam Mohamed)

URL: [cristina.dieecs.com](http://cristina.dieecs.com) (Cristina-González-Morán), [arboleya.dieecs.com](http://arboleya.dieecs.com) (Pablo Arbolea)

- The large number of nodes and lines makes the impedance matrix hard to implement [12]. The node incidence matrix might be more appropriate.
- The DG controls are usually implemented in an orthogonal-stationary reference frame  $\alpha\beta 0$  [4, 9].

The algorithms based on Newton Raphson show several difficulties at distribution levels that are well documented [13]. In contrast, the algorithms based on the application of the Kirchhoff's Current Law (KCL) and the Kirchhoff's Voltage Law (KVL) present better behavior with the special characteristics of distribution systems. This is the case of one of the most successful approaches: The Backward/Forward Sweep BFS [14], based on ladder iterative techniques [15]. The BFS algorithms present computational efficiency at each iteration because, in contrast to direct methods, the system of equations is divided into different parts, so the solution is obtained without solving all the equations simultaneously.

In [16] it is demonstrated that the advantages of BFS methods are especially shown at distribution levels. However, some authors agree that the BFS algorithms show problems such as topological limitations and lack of generality (inefficient modeling of large systems, arbitrary topologies and connections of some devices, as transformers) [17].

The authors in [13] employed a BFS algorithm, but there are two issues that can be improved in their solver: first, the using of the admittance matrix, which includes all the drawbacks described in [12]. Second, the matrix formulation needs the inversion of some matrices that might be singular. This problem was overcome in [13] transforming the line to neutral voltages into sequence components. But the sequence components present two drawbacks: the inclusion of transformers with unbalanced impedances is not allowed and the zero component cannot be adequately updated for connections with no voltage reference point on at least one side of the transformer ( $\Delta$  or ungrounded Y).

The work in [18] solves the generalization problems of [13], but they formulated the power flow problem in  $abc$  frame, which does not facilitate the inclusion of DG. Besides, with the conventional  $abc$  formulation, convergence is not always achieved in many cases with several transformer connections [19, 20, 21, 22, 23, 24, 25, 26].

In the present work, an improved BFS algorithm is proposed. The algorithm applies the matrix formulation in  $\alpha\beta 0$  described in [20]. As it will be demonstrated, the proposed algorithm does not have the limitations of [13] or [18] because there is no need of admittance matrix, sequence components or singular inversions. The convergence problems of  $abc$  formulation will be also overcome.

The novelty of this work is the definition of a BFS algorithm in  $\alpha\beta 0$  reference that allows the inclusion of matrix formulation, unbalanced lines and loads, any kind of connection for three phase transformers, DG (PQ and PV nodes) and single phase laterals. There is no previous work to define a BFS algorithm including all these features.

For comparison purposes, the authors have chosen a direct approach [20, 27, 28] to solve the system of equations by means of the trust-region dogleg algorithm [29]. This algorithm and the proposed one are tested on several cases to show up the improvements in robustness, efficiency and solving time.

The contributions and improvements in the load flow problem can be summarized as follows:

- The advantages of  $\alpha\beta 0$  matrix formulation: generalization for arbitrary connections and device locations (specially transformers) and definition of radially distribution systems with DG, coupling between components and untransposed lines are exploited in a BFS solver.
- The matrix inversion problems described in [13] are solved for all transformer connections.
- Single phase laterals and PV nodes do not mean the convergence problems of direct methods.
- Only the node voltage profile has to be estimated at the beginning of the iterative process, in contrast to direct methods in which all the system unknowns must be approximated. Moreover, the algorithm convergence is not sensitive to the initial estimation accuracy.
- The BFS solver shows increased robustness and efficiency, while the computation time is widely reduced. This issue is of especial interest in real time situations in which the time reduction in power flow calculations is decisive (for instance in contingency analysis).

The paper is structured as follows. Section 2 summarizes the matrix formulation in  $\alpha\beta 0$  frame. In Section 3 the proposed algorithm is described. Section 4 presents the validation in the IEEE 4 Node and 37 Node Test Feeders [30]. The evaluation in a large system; IEEE 123 Node Test Feeder [30] is carried out in Section 5 and finally, a conclusion is given in Section 6.

	$\mathbf{I}_{B\&T}$	$\mathbf{I}_L$	$\mathbf{I}_G$	$\mathbf{V}_{nd}$
KVL (branches)	$[\mathbf{Z}_{\alpha\beta 0}]$	$[\mathbf{0}]$	$[\mathbf{0}]$	$[-\mathbf{\Gamma}]$
KCL (nodes)	$[\mathbf{\Gamma}]^T$	$[\mathbf{I}_d]$	$[-\mathbf{I}_d]$	$[\mathbf{0}]$

Figure 1: Matrix  $\mathbf{M}$ .

## 2. Load flow matrix formulation in $\alpha\beta 0$

The  $\alpha\beta 0$  to  $abc$  transformation [31] for a generic complex vector (or phasor)  $\mathbf{x}$  will be defined as:

$$\mathbf{x}_{abc} = \mathbf{A} \mathbf{x}_{\alpha\beta 0} \quad (1)$$

where  $\mathbf{A}$  is the regular matrix:

$$\mathbf{A} = \sqrt{\frac{2}{3}} \begin{pmatrix} 1 & 0 & \frac{1}{\sqrt{2}} \\ -\frac{1}{2} & \frac{\sqrt{3}}{2} & \frac{1}{\sqrt{2}} \\ -\frac{1}{2} & -\frac{\sqrt{3}}{2} & \frac{1}{\sqrt{2}} \end{pmatrix}$$

The inverse of this matrix can be easily calculated as  $\mathbf{A}^{-1} = \mathbf{A}^T$ , so the  $abc$  to  $\alpha\beta 0$  transformation is directly obtained by using  $\mathbf{A}^T$ .

The system to be solved is formed of two different groups of equations: the core network and the nodal equations. The core network equations are linear so they can be organized into a matrix equation (2):

$$\mathbf{M} \mathbf{X}^T = [\mathbf{0}] \quad (2)$$

where  $\mathbf{X}$  is a vector including all system variables [20]:

$$\mathbf{X} = [ [\mathbf{I}_{B\&T}]_{\alpha\beta 0} \quad [\mathbf{I}_L]_{\alpha\beta 0} \quad [\mathbf{I}_G]_{\alpha\beta 0} \quad [\mathbf{V}_{nd}]_{\alpha\beta 0} ] \quad (3)$$

where:

$[\mathbf{I}_{B\&T}]_{\alpha\beta 0}$  is a vector comprised of the currents through branches and transformers in  $\alpha\beta 0$ .

$[\mathbf{I}_L]_{\alpha\beta 0}$  is a vector comprised of the currents consumed by loads from nodes in  $\alpha\beta 0$ .

$[\mathbf{I}_G]_{\alpha\beta 0}$  is a vector comprised of the currents injected by generators to nodes in  $\alpha\beta 0$ .

$[\mathbf{V}_{nd}]_{\alpha\beta 0}$  is a vector comprised of the node voltages in  $\alpha\beta 0$ .

These vectors include three complex currents per branch, transformer or load and three complex voltages per node.  $\mathbf{M}$  matrix is structured as it is depicted in Figure 1.

This formulation allows the inclusion of transformer currents into the vector of branch currents, resulting in a single vector  $\mathbf{I}_{B\&T}$ . The modified node incidence matrix  $\mathbf{\Gamma}$ , the modified transposed node incidence matrix  $\mathbf{\Gamma}^T$  and the system impedance matrix in  $\alpha\beta 0$  frame  $\mathbf{Z}_{\alpha\beta 0}$  also include branches and transformers [20].  $\mathbf{I}_d$  is the identity matrix in appropriate dimensions. In this way, the transformer currents are treated as branch currents for all transformer connections and phase shifts, being the lack of generality in [17] solved.

The nodal equations are introduced by the presence of loads and generators in the system. They might be nonlinear equations and cannot be arranged in a matrix expression. Those equations vary depending on the load or generator type, as it is described in the following subsections.

### 2.1. Loads

Three different load models are usually considered: constant impedance, constant power and constant current [2]. A constant impedance load connected to node  $i$  can be modeled in  $\alpha\beta 0$  by (4).

$$[\mathbf{V}_i]_{\alpha\beta 0}^T = \mathbf{z}_{\alpha\beta 0} [\mathbf{I}_{L_i}]_{\alpha\beta 0} \quad (4)$$

$[\mathbf{V}_i]$  includes the voltages at node  $i$  and  $[\mathbf{I}_{L_i}]$  the currents demanded by the load at node  $i$ .  $\mathbf{z}_{\alpha\beta 0}$  is the load impedance, that may be unbalanced.

A constant power load ( $PQ$  type) at node  $i$  is modeled as:

$$[\mathbf{S}_i]_{\alpha\beta 0} = [\mathbf{V}_i]_{\alpha\beta 0} \circ \text{conj} [\mathbf{I}_{L_i}]_{\alpha\beta 0} \quad (5)$$

$[\mathbf{S}_i]$  is a vector including the complex powers demanded by the load at node  $i$ . The complex powers are known for a  $PQ$  load and can be balanced or unbalanced, since the operation  $\circ$  is defined as the element-wise (Hadamard) product.  $\text{conj}$  stands for conjugated operator.

Finally, a constant current load is represented by:

$$[\mathbf{I}_{L_i}]_{\alpha\beta 0} = \mathbf{A}^T \begin{bmatrix} I_a \\ I_b \\ I_c \end{bmatrix} \quad (6)$$

where  $I_a$ ,  $I_b$  and  $I_c$  are the demanded currents in  $abc$  frame, which are input data and could be unbalanced.

The data that describe the loads are usually given in terms of active and reactive powers at nominal voltage with independence of the type of load. In the algorithm, these values have to be actualized for the calculated voltages, that might be different from the nominal value, but in any case the power factor has to be kept constant.

### 2.2. Generators

Three different types of generators can be defined: slack, constant active and reactive powers ( $PQ$  type) and constant active power and voltage magnitude ( $PV$  type).

A slack generator (or slack bus) connected to node  $i$  imposes a balanced system of node voltages as shown in (7).

$$[\mathbf{V}_i]_{\alpha\beta 0} = \mathbf{A}^T \begin{bmatrix} V_{rms} e^{0j} \\ V_{rms} e^{-\frac{2\pi}{3}j} \\ V_{rms} e^{\frac{2\pi}{3}j} \end{bmatrix} \quad (7)$$

where  $V_{rms}$  is the root mean square of the specified node voltage.

A  $PQ$  generator can be added in the same way as a  $PQ$  load just by replacing  $[\mathbf{I}_{L_i}]_{\alpha\beta 0}$  by  $[\mathbf{I}_{G_i}]_{\alpha\beta 0}$  into (5).

Finally, a  $PV$  generator connected to node  $i$  is modeled by two equations: equation (8) to account for the active power specification and equation (9) for voltages:

$$\text{real}([\mathbf{V}_i]_{\alpha\beta 0} \circ \text{conj} [\mathbf{I}_{G_i}]_{\alpha\beta 0}) = \begin{bmatrix} P_a \\ P_b \\ P_c \end{bmatrix} \quad (8)$$

$$\text{abs}(\mathbf{A}[\mathbf{V}_i]_{\alpha\beta 0}) = \begin{bmatrix} V_{rms} \\ V_{rms} \\ V_{rms} \end{bmatrix} \quad (9)$$

where  $P_a$ ,  $P_b$  and  $P_c$  are the active powers and  $\text{real}$  and  $\text{abs}$  stand for real part and modulus of a complex vector respectively.

### 2.3. Single Phase Laterals

Although all the elements in the network are firstly treated as three phase elements, if a single phase element is included, the currents through the non existing phases can be directly set to zero during the calculation process, as it will be described in next section.

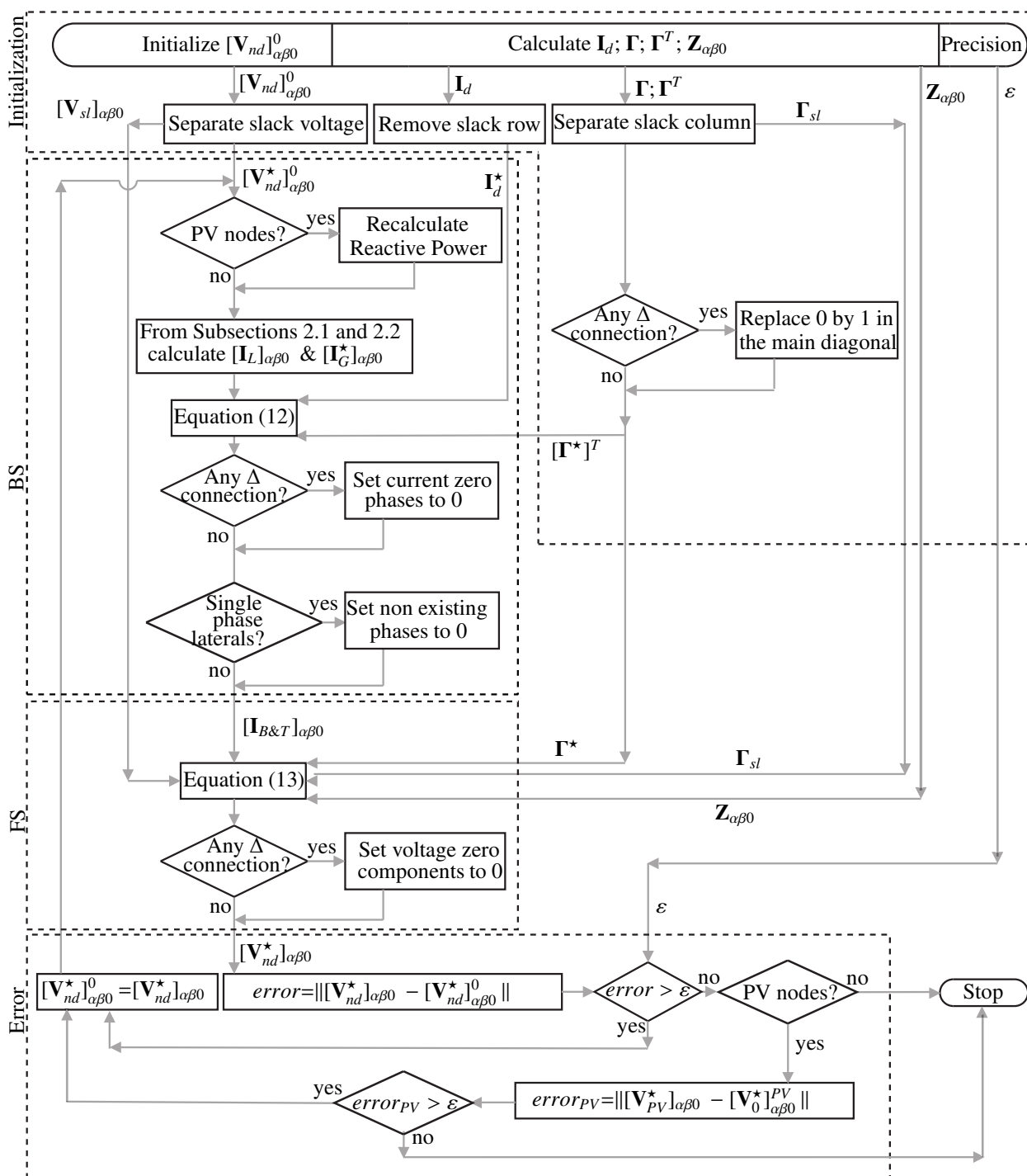


Figure 2: BFS algorithm. Flowchart.

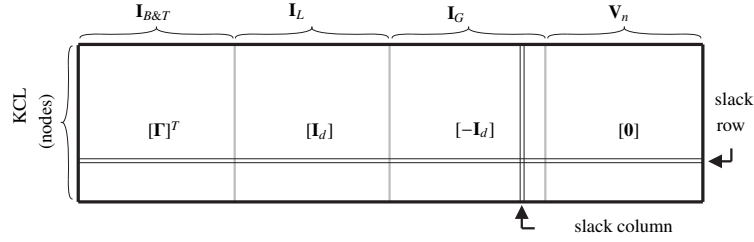


Figure 3: Backward Sweep: KCL.

### 3. Algorithm definition

The algorithm description is organized into four steps: Initialization, Backward Sweep, Forward Sweep and Error calculation. Each step is described in subsequent subsections. The whole iterative process is summarized in the flowchart of Figure 2.

A BFS algorithm is a numerical solving method conceived as an iterative process in which each iteration is split into two steps; the backward sweep and the forward sweep (BS/FS). At each step KCL or KVL equations are applied. The variables involved are divided into two groups; voltages and currents. For the first iteration, an initial voltage profile is assumed (generally a plain voltage profile). Using the initial voltages, all currents are calculated by means of the BS step. Then, the calculated currents are used for updating the voltage values in the FS step, and then the iterative process will continue until the stopping criterion is fulfilled [32].

In the proposed algorithm, the node voltages are estimated to calculate the branch currents in the BS step by means of KCL and then, the calculated currents are introduced in the KVL to update the node voltages in the FS step.

The algorithm is presented for radial networks with a slack node,  $PQ$  and  $PV$  generators and loads that can be constant impedance, constant power or constant current type, as it was described in subsection 2.1.

#### 3.1. Initialization

The input data are matrices  $\mathbf{Z}_{\alpha\beta 0}$ ,  $\mathbf{I}_d$ ,  $\mathbf{\Gamma}$  and  $\mathbf{\Gamma}^T$  (Figure 1), the slack voltages  $[\mathbf{V}_{sl}]_{\alpha\beta 0}$ , and the required precision for the iterative process  $\varepsilon$ .

The total number of variables involved in the problem (currents and voltages) depend on the number of lines (branches), transformers and nodes. It can be stated that the total number of variables is:

$$n_{var} = 3(n_B + n_T) + 3(n_L + n_G + n_{nd}) \quad (10)$$

being  $n_{var}$ ,  $n_B$ ,  $n_T$ ,  $n_L$ ,  $n_G$ ,  $n_{nd}$  the number of variables, branches, transformers, loads, generators and nodes respectively. Each line, transformer, load or generator introduces 3 variables (the three  $\alpha\beta 0$  current complex) and each node introduces other 3 variables more (the three  $\alpha\beta 0$  node voltage complex components).

The unknowns are all node voltages; so the initialization consists on assuming the node voltages  $[\mathbf{V}_{nd}]_{\alpha\beta 0}$  in (3). In this case a flat voltage profile will be considered: all system nodes have the same voltage level as the slack bus. The initial estimation will be labeled as  $[\mathbf{V}_{nd}]_{\alpha\beta 0}^0$ .

For the sake of simplicity and generalization, it is considered that there is a load and a generator per node when defining the matrix formulation in (2) and Figure 1. Then, to account for the nodes in which there is no actual connected load, the load currents are directly set to zero at the beginning of the iterative process. The same procedure is applied to generators. Due to the fact that these currents are set to zero only once before the first iteration, this procedure does not affect the computational time but it rather simplifies the matrix formulation definition. For instance, if a new generator or load is connected to or disconnected from a given network, the matrix dimensions in Figure 1 and the number of equations in (2) do not change.

#### 3.2. Backward Sweep

The Backward Sweep (BS) consists on solving the KCL equations applied to all system nodes. In the defined matrix formulation this step corresponds to the bottom of matrix  $\mathbf{M}$  (shown in Figure 3). The number of complex equations is then 3 times the number of nodes.

Being the voltage profile  $[\mathbf{V}_{nd}]_{\alpha\beta 0}^0$  estimated, then all the load currents are calculated by applying one of (4), (5) or (6), depending on the load nature. At this point the vector  $[\mathbf{I}_L]_{\alpha\beta 0}$  is known. In a similar way, the  $PQ$  type generator currents  $[\mathbf{I}_G]_{\alpha\beta 0}$  might be calculated from (5) by replacing  $[\mathbf{I}_L]_{\alpha\beta 0}$  by  $[\mathbf{I}_G]_{\alpha\beta 0}$ .

To include PV generators in the BFS solver a procedure similar to the one describe in [33] has been adopted; In a PV node the active power is known and the reactive power is set to zero at the first iteration. Then, for subsequent iterations the reactive power is recalculated considering the mismatch between the actual node voltage and the preset node voltage. The equation that defines the reactive power recalculation is as follows:

$$Q_{new} = Q_{old} - k \cdot (V_{ref}^{PV} - V_j) \quad (11)$$

where  $Q_{new}$  is the recalculated reactive power,  $Q_{old}$  the reactive power from the previous iteration and  $V_{ref}^{PV}$  and  $V_j$  are the preset voltage and the calculated voltage respectively. The factor  $k$  is a damping factor that has been included to improve the calculation time. This factor can be changed from one iteration to the next, as the mismatch between voltages improves.

Once the reactive power  $Q_{new}$  is obtained, as the active power is fixed, from here the PV generator can be treated as a PQ generator. This step is reflected in the flowchart of Figure 2. At this point, the vector  $[\mathbf{I}_G]_{\alpha\beta 0}$  in (3) is known with exception of slack node currents.

In the BS step, only the currents are involved, so if  $[\mathbf{I}_L]_{\alpha\beta 0}$  and  $[\mathbf{I}_G]_{\alpha\beta 0}$  (except slack generator) are known, the number of unknowns is  $3(n_B + n_T + 1)$  (line currents, transformer currents and slack currents). In case of a radial networks the number of nodes is higher than the number of branches / transformers (more specifically  $n_{nd} = n_B + n_T + 1$ ), so the number of KCL equations is  $3n_{nd}$ , that is the same as the number of unknowns.

To obtain the matrix formulation in which only a matrix equation has to be solved, one complex equation has to be removed from the KCL matrix equation in Figure 3. The slack node is chosen as the removed equation (a row in Figure 3). The slack currents only appear in that equation, so if the indicated column is also removed, then the modified vector  $[\mathbf{I}_G^*]_{\alpha\beta 0}$  is completely known and the modified matrix  $[\mathbf{\Gamma}^*]^T$  is squared. Then, the vector  $[\mathbf{I}_{B\&T}]_{\alpha\beta 0}$  can be directly obtained:

$$[\mathbf{I}_{B\&T}]_{\alpha\beta 0} = -([\mathbf{\Gamma}^*]^T)^{-1} (\mathbf{I}_d^* [\mathbf{I}_L]_{\alpha\beta 0} - \mathbf{I}_d^* [\mathbf{I}_G^*]_{\alpha\beta 0}) \quad (12)$$

It has to be remarked that the matrix  $\mathbf{\Gamma}^*$  and the vector  $[\mathbf{I}_G^*]_{\alpha\beta 0}$  were modified as shown in Figure 3. The superscript  $*$  indicates that the slack node equations were removed.

As it can be deduced from (12), the modified matrix  $\mathbf{\Gamma}^*$  (node incidence matrix, including transformers) must be regular. This is not the case when there is at least one transformer with a 3-wire connection (delta or ungrounded wye): A 3-wire connection in  $\alpha\beta 0$  frame gives rise to a zero in the main diagonal of  $\mathbf{\Gamma}^*$  [20]. This zero appears at the position of the zero component of the current at the transformer side with a 3-wire connection. This problem can be easily detected because the zero component of the current in a 3-wire connection is always equal to zero, so it is not an actual unknown. In  $\alpha\beta 0$  frame the zero component of currents is always available so the problem can be easily avoided and solved in three steps: 1) an element different from zero (1 for instance) is used to replace the zeros in the main diagonal. Then,  $\mathbf{\Gamma}^*$  becomes regular; 2) equation (12) is solved to obtain  $[\mathbf{I}_{B\&T}]_{\alpha\beta 0}$ ; 3) the zero component of currents in  $[\mathbf{I}_{B\&T}]_{\alpha\beta 0}$  is set to zero at the corresponding positions. This solution has proved to work with any kind of transformer connection and phase shift, solving the lack of generalization of [13].

The last part of the BS step corresponds to the two phases or single phase laterals. If there are two phases or single phase elements in the network, the currents through the non existing phases are set to zero at this point.

The BS output is the vector of line and transformer currents  $[\mathbf{I}_{B\&T}]_{\alpha\beta 0}$ .

### 3.3. Forward Sweep

The Forward Sweep (FS) consists on solving the KVL equations applied to all system branches (the transformers are also included). This implies solving the top of matrix equation in (2). The FS step matrix is shown apart in Figure 4.

In this case, the number of complex equations is 3 times the number of branches, including transformers:  $3(n_B + n_T)$ . The inputs are the branch and transformer currents calculated in the BS step  $[\mathbf{I}_{B\&T}]_{\alpha\beta 0}$ . Analyzing Figure 4, it is deduced that the node voltages can be calculated from branch and transformer currents because, although the number of branches in a radial network is the number of nodes minus one ( $n_{nd} - 1$ ), the slack voltage is known, so it can be

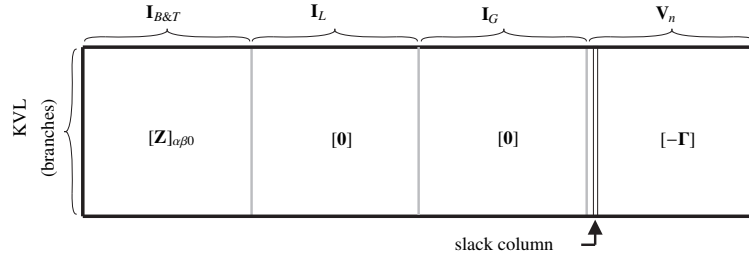


Figure 4: Forward Sweep: KVL.

eliminated from the list of unknowns (in Figure 4 a column is eliminated). The voltage profile (with exception of slack voltages) is obtained from:

$$[\mathbf{V}_{nd}^*]_{\alpha\beta 0} = -[\mathbf{\Gamma}^*]^{-1}(-\mathbf{Z}_{\alpha\beta 0} [\mathbf{I}_{B\&T}] + \mathbf{\Gamma}_{sl}[\mathbf{V}_{sl}]_{\alpha\beta 0}) \quad (13)$$

The slack column (as it is displayed in Figure 4) has been taken and passed to the other equation term. Matrix  $\mathbf{\Gamma}$  and vector  $[\mathbf{V}_{nd}]_{\alpha\beta 0}$  have been also modified accordingly.

The modified matrix  $\mathbf{\Gamma}^*$  has to be regular, and this is not possible if there is at least a 3-wire connection, as it was previously mentioned. The problem is solved in the same way as in subsection 3.2: The matrix  $\mathbf{\Gamma}^*$  is forced to be regular by replacing zeros by ones in the main diagonal when needed. Then, the voltage zero components are forced to be zero since they are not actual unknowns.

As in the BS, in the FS step only a matrix equation (equation (13)) needs to be solved. The FS step gives the vector of node voltages  $[\mathbf{V}_{nd}^*]_{\alpha\beta 0}$ .

There is a specific case in which zero components may appear in line-to-line voltages in three wire connections. This is not a feasible solution of the power flow problem. It is caused by the presence of  $Y_g\Delta$  connections and unbalanced loads simultaneously. With the defined algorithm, there will be non-zero current component nor in the transformer secondary or in the primary, so the zero component appears in voltage, when it should not be. This problem is easily detected and can be always overcome when needed by calculating the actual transformer zero current component from the corresponding KVL equation. When the actual zero current component is computed the zero voltage component disappears giving rise to a feasible solution.

As it has been demonstrated, in both BS and FS steps, the  $\alpha\beta 0$  frame facilitates the identification and solving of all the issues related to zero components in currents or voltages: singularities in the matrices and wrong voltage zero components.

### 3.4. Error calculation

The FS step output is the vector of obtained node voltages  $[\mathbf{V}_{nd}^*]_{\alpha\beta 0}$ . To calculate the error, this vector is compared with the initial estimation in case of the first iteration, or with the previous calculated voltages in case of subsequent iterations. The error is used as the stopping criterion. The iterative process stops when the error is less than the required precision. For solving PV nodes, an additional error, called  $error_{PV}$  has to be computed and included as an additional stopping criterion. In this way, the voltage at the PV nodes is forced to be equal to the preset value. If the error is higher than the precision, then the vector of estimated voltages is updated to the last calculated value. An increasing error would indicate that the problem is not convergent. This last step can be represented as shown in Figure 2.

Other stopping criteria might be implemented, for instance maximum number of allowed iterations.

## 4. Validation

The proposed BFS solver has been implemented with MATLAB software. The algorithm has been tested for validation in the IEEE 4 Node Test Feeder (in figure 5) and the IEEE 37 Node Test Feeder (in figure 6). The IEEE 4 Node feeder is the most appropriate to test all three phase transformer connections while the IEEE 37 Node feeder is a three-wire delta system with very unbalanced loading; The input data can be obtained from [30]. For comparison purposes, the authors have chosen a direct approach to simultaneously solve the whole system of equations by means



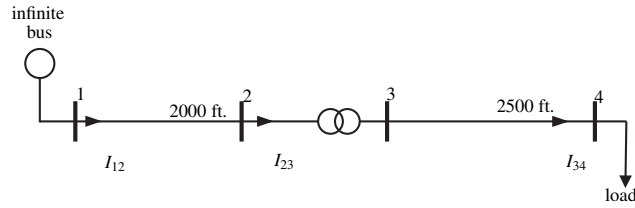


Figure 5: 4 Node Test Feeder.

Table 1: Test results IEEE 4 Node Test Feeder: Step-down Unbalanced Loading.

CONNECTION	$Y_g Y_g$	$Y_g \Delta$	$Y \Delta$	$\Delta Y_g$	$\Delta \Delta$
<b>Computation time (s)</b>					
<i>Direct Method</i>	0.896	0.725	0.787	0.743	0.753
<i>BFS</i>	0.037	0.038	0.038	0.040	0.038
<b>Number of iterations</b>					
<i>Direct Method</i>	13	6	6	7	6
<i>BFS</i>	28	14	15	27	14
<b>Current <math>I_{12}</math></b>					
$I_a$	$230.1 \angle -35.9^\circ$	$308.5 \angle -41.5^\circ$	$309.8 \angle -41.7^\circ$	$285.6 \angle -27.6^\circ$	$361.7 \angle -41.0^\circ$
$I_b$	$345.7 \angle -152.6^\circ$	$314.7 \angle -145.5^\circ$	$315.6 \angle -145.2^\circ$	$402.7 \angle -149.6^\circ$	$283.5 \angle -153.0^\circ$
$I_c$	$455.1 \angle 84.7^\circ$	$389.0 \angle 85.9^\circ$	$387.2 \angle 85.9^\circ$	$349.2 \angle 74.4^\circ$	$366.5 \angle 93.2^\circ$
<b>Current <math>I_{34}</math></b>					
$I_a$	$689.7 \angle -35.9^\circ$	$1083.9 \angle -71.0^\circ$	$1083.9 \angle -71.0^\circ$	$695.5 \angle -66.0^\circ$	$1084.1 \angle -41.0^\circ$
$I_b$	$1036.3 \angle -152.6^\circ$	$849.9 \angle 177.0^\circ$	$849.9 \angle 177.0^\circ$	$1033.0 \angle 177.1^\circ$	$849.7 \angle -153.0^\circ$
$I_c$	$1364.2 \angle 84.7^\circ$	$1098.7 \angle 63.1^\circ$	$1098.7 \angle 63.1^\circ$	$1351.9 \angle 55.2^\circ$	$1098.7 \angle 93.2^\circ$

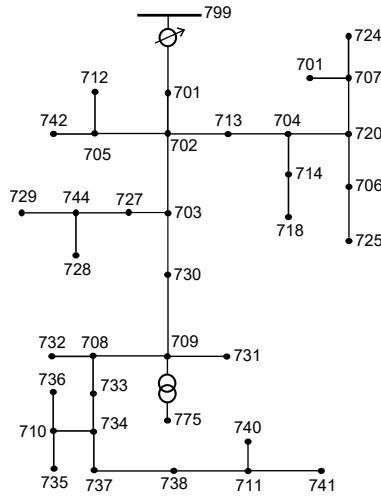


Figure 6: 37 Node Test Feeder.

of the trust-region dogleg algorithm [29]. The function *fsolve* of MATLAB software (optimization toolbox) was used as the direct method [34].

The precision for the iterative process in both cases was selected as  $\varepsilon = 10^{-4}$ . This precision satisfies the condition of error less than 0.05% as it was established in [30] by the Distribution Test Feeder Working Group. For the IEEE 4 Node Test Feeder all balanced and unbalanced loading cases as well as all step-down and step-up transformer connections were validated. Also the IEEE 37 Node Feeder was tested. Accurate results (the same for both algorithms) were obtained in all cases.

As an example, the results for all step-down connections under unbalanced loading are displayed in Table 1 (for simplicity, only the line currents were included), while the results obtained for the IEEE 37 Node Feeder are shown

Table 2: Test results IEEE 37 Node Test Feeder.

		Time (s)				
		<i>Direct Method</i>		39.852		
		<i>BFS</i>		0.075		
		Iterations				
		<i>Direct Method</i>		5		
		<i>BFS</i>		4		
Node	701	702	703	704	705	706
$V_{ab}$ (pu)	1.0317∠ - 0.08°	1.0248∠ - 0.14°	1.0178∠ - 0.18°	1.0217∠ - 0.18°	1.0241∠ - 0.13°	1.0204∠ - 0.22°
$V_{bc}$ (pu)	1.0144∠ - 120.39°	1.0088∠ - 120.58	1.0050∠ - 120.70°	1.0044∠ - 120.61°	1.0075∠ - 120.60°	1.0006∠ - 120.66°
$V_{ca}$ (pu)	1.0183∠120.61°	1.0100∠120.43°	1.0034∠120.20°	1.0064∠120.46°	1.0087∠120.46°	1.0039∠120.54°
Node	707	708	709	710	711	712
$V_{ab}$ (pu)	1.0187∠ - 0.30°	1.0086∠ - 0.08°	1.0111∠ - 0.11°	1.0024∠0.01°	0.9982∠0.06°	1.0240∠ - 0.12°
$V_{bc}$ (pu)	0.9959∠ - 120.62°	1.0002∠ - 120.73°	1.0012∠ - 120.73°	0.9967∠ - 120.76°	0.9962∠ - 120.74°	1.0073∠ - 120.61°
$V_{ca}$ (pu)	1.0024∠120.67°	0.9944∠120.02°	0.9966∠120.08°	0.9877∠119.91°	0.9851∠119.76°	1.0081∠120.46°
Node	713	714	718	720	722	724
$V_{ab}$ (pu)	1.0234∠ - 0.15°	1.0214∠ - 0.18°	1.0201∠ - 0.17°	1.0205∠ - 0.21°	1.0185∠ - 0.31°	1.0183∠ - 0.32°
$V_{bc}$ (pu)	1.0069∠ - 120.60°	1.0043∠ - 120.61°	1.0041∠ - 120.57°	1.0011∠ - 120.66°	0.9953∠ - 120.62°	0.9949∠ - 120.61°
$V_{ca}$ (pu)	1.0082∠120.44°	1.0063∠120.46°	1.0059∠120.43°	1.0040∠120.53°	1.0023∠120.69°	1.0023∠120.70°
Node	725	727	728	729	730	731
$V_{ab}$ (pu)	1.0202∠ - 0.23°	1.0167∠ - 0.16°	1.0156∠ - 0.16°	1.0156∠ - 0.16°	1.0127∠ - 0.12°	1.0109∠ - 0.13°
$V_{bc}$ (pu)	1.0003∠ - 120.66°	1.0044∠ - 120.69°	1.0036∠ - 120.68°	1.0039∠ - 120.67°	1.0021∠ - 120.73°	1.0003∠ - 120.74°
$V_{ca}$ (pu)	1.0038∠120.55°	1.0024∠120.19°	1.0016∠120.18°	1.0019∠120.17°	0.9981∠120.11°	0.9963∠120.10°
Node	732	733	734	735	736	737
$V_{ab}$ (pu)	1.0086∠ - 0.07°	1.0063∠ - 0.06°	1.0029∠ - 0.01°	1.0023∠0.03°	1.0018∠ - 0.02°	0.9996∠0.02°
$V_{bc}$ (pu)	1.0000∠ - 120.74°	0.9992∠ - 120.73°	0.9977∠ - 120.74°	0.9965∠ - 120.78°	0.9951∠ - 120.75°	0.9968∠ - 120.71°
$V_{ca}$ (pu)	0.9940∠120.02°	0.9925∠119.96°	0.9892∠119.89°	0.9872∠119.92°	0.9874∠119.96°	0.9871∠119.79°
Node	738	740	741	742	744	775
$V_{ab}$ (pu)	0.9984∠0.04°	0.9980∠0.07°	0.9981∠0.07°	1.0238∠ - 0.15°	1.0160∠ - 0.16°	1.0111∠ - 0.11°
$V_{bc}$ (pu)	0.9964∠ - 120.71°	0.9961∠ - 120.75°	0.9962∠ - 120.75°	1.0067∠ - 120.59°	1.0040∠ - 120.68°	1.0012∠ - 120.73°
$V_{ca}$ (pu)	0.9860∠119.77°	0.9846∠119.76°	0.9848∠119.76°	1.0086∠119.48°	1.0020∠120.18°	0.9966∠120.08°

in Table 2. Both tables show the computation time and the number of iterations for both algorithms. The obtained results were the same with both methods, but although the number of iterations was almost always higher for the BFS algorithm, the computation time was widely reduced. As it will be demonstrated in next section, the improvement in computation time is of special interest for larger systems.

Besides the improvement in computational time, another remarkable difference between the BFS and the direct method is the initial assumption. In the BFS only the voltage profile had to be estimated before the first iteration. In contrast, all variables in (3) needed to be assumed at the beginning of the iterative process for the direct method. The IEEE 4 Node Test Feeder is a small system so the initial estimation has no influence over the convergence for any of the solvers. The IEEE 37 Node test feeder did not show convergence problems as well. But, as it will be proved in next section, the direct method presented convergence problems related to the initial estimation in a larger system, while the BFS convergence was not sensitive to the system dimensions.

## 5. Evaluation in a large system

The evaluation of the algorithm has been carried out in the IEEE 123 Node Test Feeder (input data from [30]).

Eleven different cases were tested both with the BFS solver and the direct solver. Two base cases without transformers were firstly considered (cases 1 and 2), then other six cases (cases from 3 to 8) including different transformer connections and phase shifts were analyzed (see Figure 7 and Table 3, where PhSh stands for phase shift). The transformer configurations were chosen to include all types of connections and several phase shifts. The connections in the same studied case have to be consistent. For instance, once the connection for T1 is chosen ( $\Delta Y_g$  in configuration 2), the primary side of T2 and T3 are also fixed ( $Y_g$  in configuration 2).

Cases from 1 to 8 are summarized in Table 4, where Bal., Unbal. and Trafo Conf. stand for balanced loading, unbalanced loading and transformer configuration respectively.

Other three cases were studied; case 9 including the single phase laterals and the loading scenario described in [30], case 10, with the same scenario as case 9 but also including 8 DG units (PQ type generators). In this case, the loads in [30] were replaced by DG units in several nodes, as shown in Table 5. There are 6 single phase PQ type DG

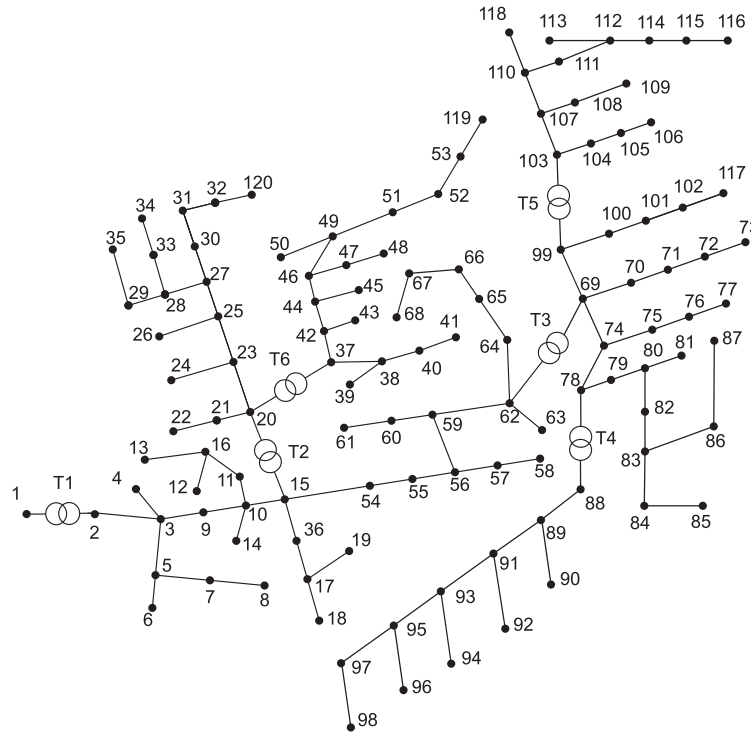


Figure 7: IEEE 123 Node Test Feeder with transformers.

Table 3: Transformers configurations.

	Configuration 1		Configuration 2		Configuration 3	
	Connection	PhSh	Connection	PhSh	Connection	PhSh
T1	YgYg	0	$\Delta Y_g$	150	$\Delta\Delta$	180
T2	YgYg	0	$Y_g\Delta$	-30	$\Delta Y_g$	-30
T3	YgYg	0	$Y_g\Delta$	150	$Y\Delta$	150
T4	YgYg	0	$\Delta\Delta$	0	$\Delta Y_g$	150
T5	YgYg	0	$Y\Delta$	150	$\Delta\Delta$	0
T6	YgYg	0	$\Delta\Delta$	180	$Y_g Y_g$	0

Table 4: Tests in the IEEE 123 Node Test Feeder.

Case	1	2	3	4	5	6	7	8
Trafo Conf.	base	base	1	1	2	2	3	3
Load Scenario	Bal.	Unb.	Bal.	Unb.	Bal.	Unb.	Bal.	Unb.

Table 5: DG locations and configurations for case 10.

Node	24	34	35	50	78	84	98	105
Configuration	BN	CN	AN	ABCN	ABCN	AN	BN	CN

units and 2 three phase PQ type DG units. The nominal power was selected to be the same as the eliminated loads. Finally, case 11 is for PV node testing; it is a similar case to case 10, but the PQ generator in node 50 was replaced by a PV node. The selected active power was kept the same while for the voltage reference 0.95 p.u. per phase is fixed. A dumping factor in (11) of  $k = 3.2$  helped to reduce computation time.

Table 6 shows the results obtained in all cases. In both algorithms the initial estimation is based on the same voltage profile: the slack node voltage applied to all system nodes. For the direct method also line and transformer currents are needed, so they are chosen to be zero.

The results in Table 6 show that in all the studied cases the differences between the direct and the BFS methods

Table 6: Test results IEEE 123 Node Test Bus Feeder.

CASE	1	2	3	4	5	6	7	8	9	10	11
Transformer Configuration	base	base	1	1	2	2	3	3	–	–	
Loading Scenario	Bal.	Unbal.	Bal.	Unbal.	Bal.	Unbal.	Bal.	Unbal.	Single Phase	DG	PV nodes
<b>Computation time (s)</b>											
<i>Direct Method</i>	341.27	299.97	367.43	346.66	1506.60	1493.40	1753.90	1772.90	3679.90	3918.10	2867.5
<i>BFS</i>	0.434	0.397	0.791	0.478	0.647	0.691	1.103	0.704	0.396	0.310	0.469
<b>Number of iterations</b>											
<i>Direct Method</i>	6	6	7	7	30	30	37	37	121	125	53
<i>BFS</i>	11	10	16	13	12	12	22	13	12	9	15
<b>Convergence Problems</b>											
<i>Direct Method</i>	no	no	no	no	yes	yes	yes	yes	yes	yes	yes
<i>BFS</i>	no	no	no	no	no	no	no	no	no	no	no

are more than remarkable. First of all, in cases from 1 to 4 both algorithms present adequate convergence for the proposed precision and initial assumptions, but the computational time for the BFS solver is much more reduced. On the other hand, in cases from 5 to 8 (these cases present delta type transformer connections) the direct method does not converge to a solution, while the BFS solver always finds a proper root.

The convergence problems in direct methods might be solved with an initial estimation closer to the solution, but this issue is not easy especially for large systems because all currents and voltages have to be assumed. Another possibility might be to reduce the precision, but the solution goodness decreases.

The computational time wasted to detect convergence problems in cases from 1 to 8 (that is the time indicated in Table 6), plus the additional time spent on selecting an appropriated initial estimation are much larger for the direct method. It has been proved that this problem is always overcome with the proposed BFS solver because the method is not sensitive to neither the precision nor the initial estimation, being convergence assured in all the studied cases.

In cases 9, 10 and 11 the advantages of the proposed method are more outstanding. The reason is the presence of single phase laterals. In direct methods, single phases and PV nodes imply ill conditioned problems that are avoided with the proposed algorithm.

## 6. Conclusion

A Backward/Forward Sweep solver for unbalanced power flow calculations has been defined in  $\alpha\beta 0$  frame using matrix formulation. The solver has shown accurate results in large distribution systems for all three phase transformer connections, single phase laterals and distributed generators, while the problems related to Backward/Forward Sweep solvers presented in the literature have been solved; the  $\alpha\beta 0$  frame facilitates the identification and solving of all the issues related to zero components in currents or voltages.

When compared to a direct method the computation time is reduced avoiding convergence problems. The main improvements reside in the simplicity of the initial estimation and the inclusion of single phase laterals. In the proposed solver only the voltage profile has to be estimated at the beginning of the iterative process, in contrast to direct methods in which also the currents have to be assumed. When single phase laterals are present the algorithm does not show ill conditioned problems. These advantages give rise to a much more robust convergence for the proposed solver. The improvements are especially visible for large systems.

Summarizing, it has been proved that the algorithm is general, robust and computational saving.

## References

- [1] A. Keane, L. Ochoa, C. Borges, G. Ault, A. Alarcon-Rodriguez, R. Currie, F. Pilo, C. Dent, G. Harrison, State-of-the-art techniques and challenges ahead for distributed generation planning and optimization, *IEEE Trans. Power Syst.* 28 (2) (2013) 1493–1502.
- [2] Ieee recommended practice for industrial and commercial power systems analysis (brown book) (Aug 1998).
- [3] G. Chang, S.-Y. Chu, M.-F. Hsu, C.-S. Chuang, H.-L. Wang, An efficient power flow algorithm for weakly meshed distribution systems, *Elect. Power Syst. Res.* 84 (1) (2012) 90 – 99.
- [4] M. Kamh, R. Iravani, Unbalanced model and power-flow analysis of microgrids and active distribution systems, *IEEE Trans. Power Del.* 25 (4) (2010) 2851 –2858.
- [5] J.-H. Teng, A direct approach for distribution system load flow solutions, *IEEE Trans. Power Del.* 18 (3) (2003) 882 – 887.

- [6] M. Golsorkhi, D. Lu, A control method for inverter-based islanded microgrids based on v-i droop characteristics, *IEEE Trans. Power Del.* PP (99) (2014) 1–1.
- [7] J. Vasquez, J. Guerrero, M. Savaghebi, J. Eloy-Garcia, R. Teodorescu, Modeling, analysis, and design of stationary-reference-frame droop-controlled parallel three-phase voltage source inverters, *IEEE Trans. Ind. Electron.* 60 (4) (2013) 1271–1280.
- [8] L. Meng, F. Tang, M. Savaghebi, J. Vasquez, J. Guerrero, Tertiary control of voltage unbalance compensation for optimal power quality in islanded microgrids, *IEEE Trans. Energy Convers.* 29 (4) (2014) 802–815.
- [9] M. Kamh, R. Iravani, Steady-state model and power-flow analysis of single-phase electronically coupled distributed energy resources, *IEEE Trans. Power Del.* 27 (1) (2012) 131–139.
- [10] S. Jankovic, B. Ivanovic, Application of combined newton-raphson method to large load flow models, *Elect. Power Syst. Res.* 127 (2015) 134–140.
- [11] W. Kersting, W. Phillips, Distribution feeder line models, *IEEE Trans. Ind. Applicat.* 31 (4) (1995) 715–720.
- [12] F. Milano, *Power System Modelling and Scripting*, Springer, 2010.
- [13] P. Xiao, D. Yu, W. Yan, A unified three-phase transformer model for distribution load flow calculations, *IEEE Trans. Power Syst.* 21 (1) (2006) 153–159.
- [14] W. H. Kersting, *Distribution System Modeling and Analysis*, CRC Press, Abingdon, 2001.
- [15] W. Kersting, A method to teach the design and operation of a distribution system, *IEEE Power Engineering Review PER-4* (7) (1984) 72–72.
- [16] L. Araujo, D. R. R. Penido, S. Carneiro, J. L. R. Pereira, P. A. N. Garcia, A comparative study on the performance of tcim full newton versus backward-forward power flow methods for large distribution systems, in: *Power Systems Conference and Exposition, 2006. PSCE '06. 2006 IEEE PES, 2006*, pp. 522–526.
- [17] I. Kocar, J. Mahseredjian, U. Karaagac, G. Soykan, O. Saad, Multiphase load-flow solution for large-scale distribution systems using mana, *IEEE Trans. Power Del.* 29 (2) (2014) 908–915.
- [18] L. Kocar, J.-S. Lacroix, Implementation of a modified augmented nodal analysis based transformer model into the backward forward sweep solver, *IEEE Trans. Power Syst.* 27 (2) (2012) 663–670.
- [19] R. R. Mojumdar, P. Arboleya, C. Gonzalez-Morn, Step-voltage regulator model test system, in: *2015 IEEE Power Energy Society General Meeting, 2015*, pp. 1–5. doi:10.1109/PESGM.2015.7286097.
- [20] P. Arboleya, C. Gonzalez-Moran, M. Coto, Unbalanced power flow in distribution systems with embedded transformers using the complex theory in  $\alpha\beta 0$  stationary reference frame, *IEEE Trans. Power Syst.* PP (99) (2014) 1–11.
- [21] W. H. Kersting, W. H. Phillips, W. Carr, A new approach to modeling three-phase transformer connections, *IEEE Transactions on Industry Applications* 35 (1) (1999) 169–175. doi:10.1109/28.740861.
- [22] R. C. Dugan, A perspective on transformer modeling for distribution system analysis, in: *2003 IEEE Power Engineering Society General Meeting (IEEE Cat. No.03CH37491)*, Vol. 1, 2003, p. 119 Vol. 1. doi:10.1109/PES.2003.1267146.
- [23] T. H. Chen, M. S. Chen, T. Inoue, P. Kotas, E. A. Chebli, Three-phase cogenerator and transformer models for distribution system analysis, *IEEE Transactions on Power Delivery* 6 (4) (1991) 1671–1681. doi:10.1109/61.97706.
- [24] M. R. Irving, A. K. Al-Othman, Admittance matrix models of three-phase transformers with various neutral grounding configurations, *IEEE Transactions on Power Systems* 18 (3) (2003) 1210–1212. doi:10.1109/TPWRS.2003.814905.
- [25] M. E. Baran, E. A. Staton, Distribution transformer models for branch current based feeder analysis, *IEEE Transactions on Power Systems* 12 (2) (1997) 698–703. doi:10.1109/59.589655.
- [26] Z. Wang, F. Chen, J. Li, Implementing transformer nodal admittance matrices into backward/forward sweep-based power flow analysis for unbalanced radial distribution systems, *IEEE Transactions on Power Systems* 19 (4) (2004) 1831–1836. doi:10.1109/TPWRS.2004.835659.
- [27] G. Diaz, C. Gonzalez-Moran, Fischer-burmeister-based method for calculating equilibrium points of droop-regulated microgrids, *IEEE Trans. Power Syst.* 27 (2) (2012) 959–967.
- [28] P. Arboleya, G. Diaz, M. Coto, Unified ac/dc power flow for traction systems: A new concept, *IEEE Trans. Veh. Technol.* PP (99) (2012) 1.
- [29] T. Steihaug, The conjugate gradient method and trust regions in large scale optimization, *SIAM Journal on Numerical Analysis* 20 (3) (1983) 626–637.
- [30] Distribution Test Feeders, IEEE PES Distribution System Analysis Subcommittee's. Distribution Test Feeder Working Group. [On-line]. Available: <http://ewh.ieee.org/soc/pes/dsacom/testfeeders/>.
- [31] G. Paap, Symmetrical components in the time domain and their application to power network calculations, *IEEE Trans. Power Syst.* 15 (2) (2000) 522–528.
- [32] G. Chang, S. Chu, H. Wang, An improved backward/forward sweep load flow algorithm for radial distribution systems, *IEEE Trans. Power Syst.* 22 (2) (2007) 882–884.
- [33] G. X. Luo, A. Semlyen, Efficient load flow for large weakly meshed networks, *IEEE Trans. Power Syst.* 5 (4) (1990) 1309–1316.
- [34] <http://www.mathworks.es/es/help/optim/ug/fsolve.html>.